

Nonlinear magneto-optical rotation of frequency-modulated light resonant with a low- J transition

Yu. P. Malakyan,^{1,*} S. M. Rochester,^{2,†} D. Budker,^{2,3,‡} D. F. Kimball,^{2,§} and V. V. Yashchuk^{2,¶}

¹*Institute for Physical Research, National Academy of Sciences of Armenia, Ashtarak-2, 378410, Armenia*

²*Department of Physics, University of California at Berkeley, Berkeley, California 94720-7300*

³*Nuclear Science Division, Lawrence Berkeley National Laboratory, Berkeley, California 94720*

(Dated: August 14, 2018)

A low-light-power theory of nonlinear magneto-optical rotation of frequency-modulated light resonant with a $J = 1 \rightarrow J' = 0$ transition is presented. The theory is developed for a Doppler-free transition, and then modified to account for Doppler broadening and velocity mixing due to collisions. The results of the theory are shown to be in qualitative agreement with experimental data obtained for the rubidium $D1$ line.

PACS numbers: 42.50.Gy, 32.80.Bx, 07.55.Ge

I. INTRODUCTION

Nonlinear magneto-optical rotation (NMOR), or light-power-dependent rotation of optical polarization due to resonant interaction with an atomic medium in the presence of a magnetic field B , has applications ranging from fundamental symmetry tests to magnetometry [1]. With

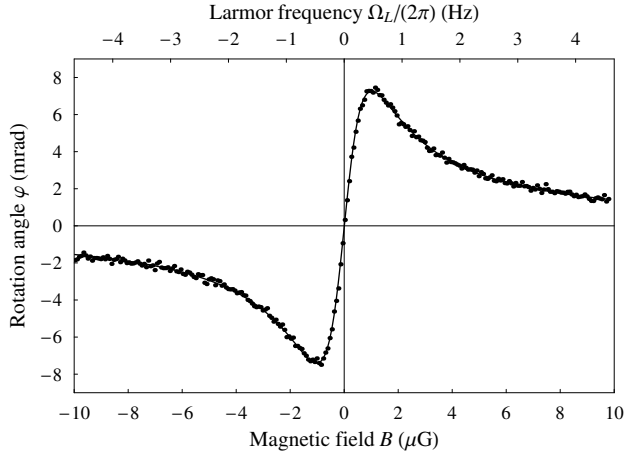


FIG. 1: Experimental (dots) and dispersive-Lorentzian least-squares fit (line) magnetic-field dependence of NMOR in a 10-cm-diameter paraffin-coated ^{85}Rb -vapor cell, obtained as described in Ref. [3]. Linearly polarized laser light is tuned to the high-frequency side of the $D2$ $F = 3 \rightarrow F'$ transition, at which maximum rotation occurs. The light intensity is $\sim 50 \mu\text{W cm}^{-2}$, and the beam diameter is ~ 2 mm. The temperature of the cell is $\sim 19^\circ\text{C}$ corresponding to a vapor density of $\sim 4 \times 10^9 \text{ cm}^{-3}$.

NMOR due to the evolution of ground-state atomic polarization [2], optical rotation is proportional to the magnetic field for small fields, but falls off when the Larmor frequency $\Omega_L = g\mu_0 B$ (g is the gyromagnetic ratio, μ_0 is the Bohr magneton, and we set $\hbar = 1$ throughout) becomes larger than half of the atomic polarization relaxation rate γ (Fig. 1). Atomic polarization relaxation rates as low as $\gamma \simeq 2\pi \times 1 \text{ Hz}$ can be achieved for alkali atoms contained in paraffin-coated vapor cells [4], corresponding to magnetic field widths of approximately $1 \mu\text{G}$ [5] and high magnetometric sensitivity ($\sim 3 \text{ pG Hz}^{-1/2}$ [3]) to small fields.

With a traditional NMOR magnetometer, the high small-field sensitivity comes at the expense of a limited dynamic range. Since many applications (such as measurement of geomagnetic fields or magnetic fields in space [6]) require high sensitivity at magnetic fields on the order of a Gauss, a method to extend the magnetometer's dynamic range is needed. It was recently demonstrated [7, 8] that when frequency-modulated light is used to induce and detect nonlinear magneto-optical rotation (FM NMOR), the narrow features in the magnetic-field dependence of optical rotation normally centered at $B = 0$ can be translated to much larger magnetic fields. In this setup (Fig. 2), the light frequency is modulated at frequency Ω_m , and the time-dependent optical rotation is measured at a harmonic of this frequency. Narrow features appear, centered at Larmor frequencies that are integer multiples of Ω_m , allowing the dynamic range of the magnetometer to extend well beyond the Earth field.

Light-frequency modulation has been previously applied to measurements of *linear* magneto-optical rotation and parity-violating optical rotation [9, 10] in order to produce a time-dependent optical rotation signal without introducing additional optical elements (such as a Faraday modulator) between the polarizer and analyzer. Optical pumping with frequency-modulated light has been applied to magnetometry with ^4He [11, 12, 13] and Cs [14]; in these experiments transmission, rather than optical rotation, was monitored. In the latter work with Cs, the modulation index (the ratio of modulation depth to modulation frequency) is on the order of unity,

*Electronic address: yumal@ipr.sci.am

†Electronic address: simonkeys@yahoo.com

‡Electronic address: budker@socrates.berkeley.edu

§Electronic address: dfk@uclink4.berkeley.edu

¶Electronic address: yashchuk@socrates.berkeley.edu

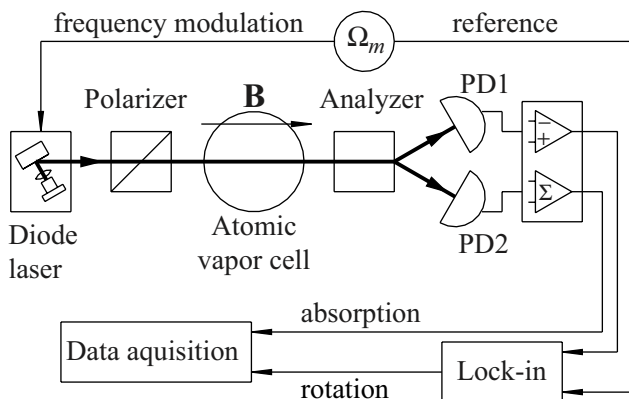


FIG. 2: Simplified schematic of the apparatus used to detect FM NMOR signals. A paraffin-coated cell containing Rb vapor is placed inside a balanced polarimeter (a polarizer and an analyzer oriented at $\sim 45^\circ$ with respect to each other). The frequency of the laser is modulated with an amplitude of a few dozen MHz. The lock-in amplifier is used to detect the components of optical rotation oscillating both in phase and $\pi/2$ out of phase with the frequency modulation.

in contrast to the much larger index in the work described here, allowing interpretation of the process in terms of the Λ - or coherent-population-trapping resonances. This regime has also been explored in Rb using modulation of the magnetic field, rather than the light field [15]. The closely related method of modulation of light intensity (synchronous optical pumping) predates the frequency-modulation technique [16]. Also employing light-intensity modulation is the so-called quantum beat resonance technique [17] used, for example, for measuring the Landé factors of molecular ground states (see Ref. [18] and references therein). Intensity modulation was recently used in experiments that put an upper limit on the (parity- and time-reversal-violating) electric dipole moment of ^{199}Hg (Refs. [19, 20] and references therein).

A quantitative theory of FM NMOR would be of use in the study and application of the technique. As a first step towards a complete theory, we present here a perturbative calculation for a $J = 1 \rightarrow J' = 0$ atomic transition that takes into account Doppler broadening and averaging due to velocity-changing collisions. We begin the discussion in Sec. II by comparing experimental FM NMOR magnetic-field-dependence data obtained with a paraffin-coated ^{87}Rb -vapor cell to the predictions of the calculation (described in Sec. III). We find that the simplified model still reproduces the salient features of the observed signals, indicating that the magnetic-field dependence of FM NMOR at low light power is not strongly dependent on power or angular momentum. As discussed in Sec. IV, the description of the saturation behavior and spectrum of FM NMOR in a system like Rb, on the other hand, will require a more complete theory.

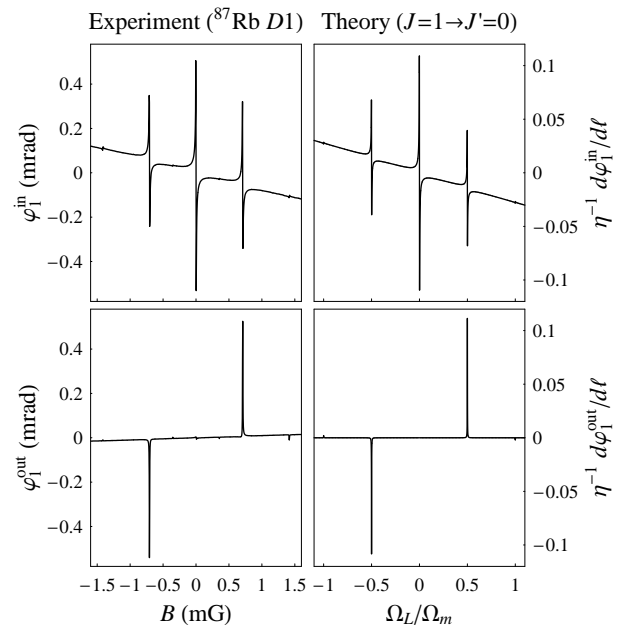


FIG. 3: Measured (left column) and calculated (right column) in-phase (top row) and quadrature (bottom row) first-harmonic amplitudes of FM NMOR. The experimental signals, plotted as a function of magnetic field B applied along the light propagation direction, are obtained with light tuned to the wing of the $F = 2 \rightarrow F' = 1$ absorption line of the ^{87}Rb $D1$ spectrum. The laser power is $15 \mu\text{W}$, beam diameter is $\sim 2 \text{ mm}$, $\Omega_m = 2\pi \times 1 \text{ kHz}$, and modulation amplitude is $2\pi \times 220 \text{ MHz}$. All resonances have widths ($\sim 1 \mu\text{G}$) corresponding to the rate of atomic polarization relaxation in the paraffin-coated cell. The normalized calculated signals [Eq. 58], for a $J = 1 \rightarrow J' = 0$ transition, are plotted as a function of normalized Larmor frequency Ω_L/Ω_m . For these plots, the parameters $\Delta_0/\Gamma_D = 0.7$, $\Omega_m/\gamma = 500$, and $\Delta_l/\Delta_0 = 1$ (described in Sec. III) are chosen to match the experimental parameters given above.

II. EXPERIMENTAL DATA AND COMPARISON WITH THEORY

Figures 3 and 4 show first- and second-harmonic data, respectively, obtained from an FM NMOR magnetometer with light tuned near the $D1$ line of rubidium in the manner described in Ref. [7, 8], along with the predicted signals for a $J = 1 \rightarrow J' = 0$ transition obtained from the theory described in Sec. III with parameters matching those of the experimental data. The calculation for the simpler system reproduces many of the qualitative aspects of the experimental data for Rb. The features at the center of the in-phase plots of Figs. 3 and 4 are the zero-field resonances, analogous to the one shown in Fig. 1. (The background linear slope seen in the in-phase signals is also a zero-field resonance, due to the “transit effect” [1]. It is modelled in the theory by an extra term analogous to the others with the isotropic relaxation rate γ equal to the transit rate of atoms through the laser beam.) In addition to these features, there appear

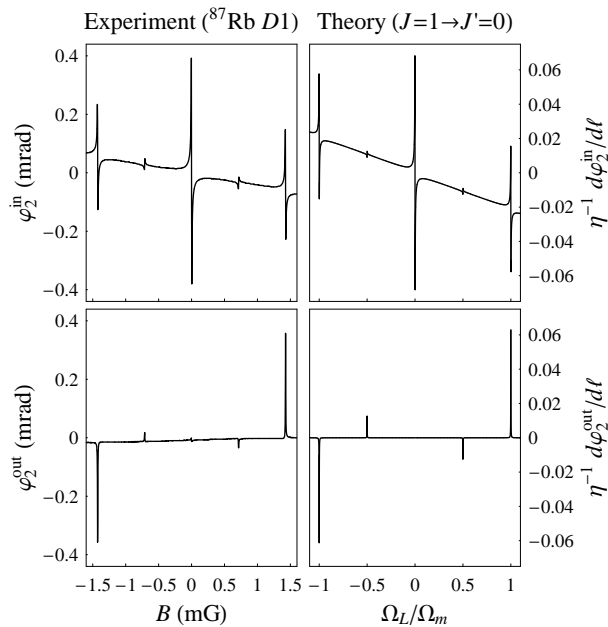


FIG. 4: Measured and calculated second-harmonic amplitudes of FM NMOR. See caption to Fig. 3. For the experimental signals, light is tuned to the center of the $F = 2 \rightarrow F' = 1$ absorption line of the ^{87}Rb D1 spectrum, the laser power is $15 \mu\text{W}$, beam diameter is $\sim 2.5 \text{ mm}$, $\Omega_m = 2\pi \times 1 \text{ kHz}$, and modulation amplitude is $2\pi \times 440 \text{ MHz}$. The parameters for the theoretical signals are $\Delta_0/\Gamma_D = 1.4$, $\Omega_m/\gamma = 500$, and $\Delta_l/\Delta_0 = 0.2$.

new features centered at magnetic field values at which $|\Omega_L/\Omega_m| = 1/2$ and 1. For the first-harmonic signal, the former are larger, whereas for the second-harmonic, the latter are; this is primarily a result of the different light detunings used in the two measurements. For these new resonances, there are both dispersively shaped in-phase signals and $\pi/2$ out of phase (quadrature) components peaked at the centers of these resonances. The resonances occur when the optical pumping rate, which is periodic with frequency Ω_m due to the laser frequency modulation, is synchronized with Larmor precession, which for an aligned state has periodicity at frequency $2\Omega_L$ as a result of the state's rotational symmetry. This results in the atomic medium being optically pumped into an aligned rotating state, modulating the optical properties of the medium at $2\Omega_L$. The aligned atoms produce maximum optical rotation when the alignment axis is at $\pi/4$ to the direction of the light polarization and no rotation when the axis is along the light polarization. Thus, on resonance, there is no in-phase signal and maximum quadrature signal. The relative sizes and signs of the features in the magnetic-field dependence, largely determined by the ratio of the modulation width Δ_0 to the Doppler width Γ_D (Sec. III), are well reproduced by the theory. The theory also exhibits the expected linear light-power dependence of the optical rotation amplitude as observed in experiments at low power [7, 8].

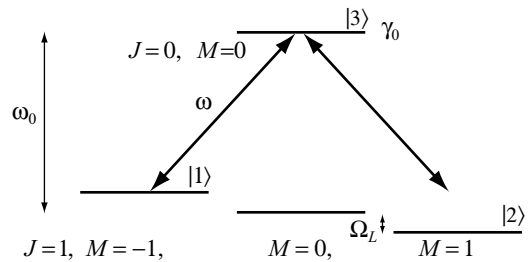


FIG. 5: A $J_g = 1 \rightarrow J_e = 0$ atomic transition of frequency ω_0 . The lower sublevels are split by the Larmor frequency Ω_L . The arrows indicate the interaction with light of frequency ω polarized perpendicular to the quantization axis. The upper state spontaneously decays a rate γ_0 .

There are additional features, centered at $|\Omega_L/\Omega_m| = 1/4$, just barely visible in the experimental plots of Figs. 3, 4. These features, which become more prominent at higher light power [8], are due to the optical pumping, precession, and detection of the hexadecapole moment. These resonances are not described by the current theory, because the presence of the hexadecapole moment requires ground-state angular momentum $J \geq 2$ and second-order light interactions. A quantitative description of these resonances is among the goals for an expanded theory.

III. THEORY

A. Introduction

The goals for a complete theory of FM NMOR are outlined in Sec. IV. As a first step towards such a theory, we calculate here the optical rotation due to interaction of frequency-modulated light with a $J_g = 1 \rightarrow J_e = 0$ atomic transition (Fig. 5), where the subscripts g and e indicate the ground and excited states, respectively. We will assume that the light power is low enough that no optical pumping saturation occurs.

We begin by calculating the time-dependent atomic ground-state coherence of a Doppler-free system. Using the magnetic-field-atom and light-atom interaction Hamiltonians (under the rotating wave approximation) we write the density-matrix evolution equations. Under the low-light-power approximation, an expression for the ground-state atomic coherence can be written as a time integral. We convert the integral to a sum over harmonics of the modulation frequency by expanding the integrand as a series. This form is convenient for this calculation because the optical rotation signal is measured by lock-in detection. The expression for the Doppler-free case is then modified to take into account Doppler broadening and velocity averaging due to collisions. Atoms in an antirelaxation-coated vapor cell collide with the cell walls in between interactions with the light beam, preserving their polarization but randomizing their veloci-

ties. In the low-light-power case, we can account for this by first calculating the effect of optical pumping assuming no collisions, and then averaging the density matrix over atomic velocity. Note that in this case we assume that optical pumping is unsaturated not only for the resonant velocity group, but also when atomic polarization is averaged over the velocity distribution and cell volume.

Using the wave equation, we find an expression for the time-dependent optical rotation in terms of the atomic ground-state coherence of a given atomic velocity group. This rotation is then integrated over time and atomic velocity to obtain an expression for the signal at a given harmonic measured by the lock-in detector.

B. The Hamiltonian

The total Hamiltonian H is the sum of the unperturbed Hamiltonian H_0 , the light-atom-interaction Hamiltonian H_l , and the magnetic-field-atom-interaction Hamiltonian H_B . Using the basis states $|\xi JM\rangle$, where ξ represents additional quantum numbers, denoted by

$$\begin{aligned} |\xi_g J_g, -1\rangle &= \begin{pmatrix} 1 \\ 0 \\ 0 \\ 0 \end{pmatrix}, & |\xi_g J_g, 0\rangle &= \begin{pmatrix} 0 \\ 1 \\ 0 \\ 0 \end{pmatrix}, \\ |\xi_g J_g, 1\rangle &= \begin{pmatrix} 0 \\ 0 \\ 1 \\ 0 \end{pmatrix}, & |\xi_e J_e, 0\rangle &= \begin{pmatrix} 0 \\ 0 \\ 0 \\ 1 \end{pmatrix}, \end{aligned} \quad (1)$$

the unperturbed Hamiltonian H_0 is given by

$$H_0 = \begin{pmatrix} 0 & 0 & 0 & 0 \\ 0 & 0 & 0 & 0 \\ 0 & 0 & 0 & 0 \\ 0 & 0 & 0 & \omega_0 \end{pmatrix}, \quad (2)$$

where ω_0 is the transition frequency (again, we set $\hbar = 1$ throughout).

An x -polarized optical electric field \mathbf{E} is written as

$$\mathbf{E} = E_0 \cos(\omega t) \hat{\mathbf{e}}_x. \quad (3)$$

where E_0 is the electric field amplitude and ω is the frequency (modulated as $\omega = \omega_l - \Delta_0 \cos \Omega_m t$, where ω_l is the laser carrier frequency and Δ_0 is the modulation amplitude). We assume that the atomic medium is optically thin, so that we can neglect the change in light polarization and intensity inside the medium when calculating the state of the medium. The light-atom interaction Hamiltonian is given by

$$\begin{aligned} H_l &= -\mathbf{E} \cdot \mathbf{d} \\ &= -E_0 \cos(\omega t) d_x \\ &= -\frac{1}{\sqrt{2}} E_0 \cos(\omega t) (d_{-1} - d_{+1}), \end{aligned} \quad (4)$$

where \mathbf{d} is the dipole operator. According to the Wigner-Eckart theorem, components of a tensor operator $T_{\kappa q}$ are related to the reduced matrix element $(\xi J \| T_{\kappa} \| \xi J')$ by [21]

$$\langle \xi J M | T_{\kappa q} | \xi' J' M' \rangle = (-1)^{J-M} (\xi J \| T_{\kappa} \| \xi' J') \begin{pmatrix} J & \kappa & J' \\ -M & q & M' \end{pmatrix}. \quad (5)$$

Thus the matrix elements of d_{+1} and d_{-1} for this transition can be written

$$\begin{aligned} \langle \xi J M | d_{\pm 1} | \xi' J' M' \rangle &= (-1)^{J-M} (\xi J \| d \| \xi' J') \begin{pmatrix} J & 1 & J' \\ -M & \pm 1 & M' \end{pmatrix} \\ &= \frac{1}{\sqrt{3}} \times \begin{cases} (\xi_e J_e \| d \| \xi_g J_g) & \text{for } \xi = \xi_e, J = J_e, M = 0 \\ & \text{and } \xi' = \xi_g, J' = J_g, M' = \mp 1, \\ (\xi_g J_g \| d \| \xi_e J_e) & \text{for } \xi = \xi_g, J = J_g, M = \pm 1 \\ & \text{and } \xi' = \xi_e, J' = J_e, M' = 0, \\ 0 & \text{in all other cases.} \end{cases} \end{aligned} \quad (6)$$

Reduced matrix elements with different ordering of states are related by [21]

$$(\xi J \| T_{\kappa} \| \xi' J') = (-1)^{J-J'} (\xi' J' \| T_{\kappa} \| \xi J)^*, \quad (7)$$

and since the reduced dipole matrix element is real,

$$(\xi_g J_g \| d \| \xi_e J_e) = -(\xi_e J_e \| d \| \xi_g J_g). \quad (8)$$

Thus H_l is given in matrix form by

$$H_l = 2\Omega \cos \omega t \begin{pmatrix} 0 & 0 & 0 & -1 \\ 0 & 0 & 0 & 0 \\ 0 & 0 & 0 & 1 \\ -1 & 0 & 1 & 0 \end{pmatrix}, \quad (9)$$

where $\Omega = (\xi_g J_g \| d \| \xi_e J_e) E_0 / (2\sqrt{6})$ is (apart from a numerical factor of order unity) the optical Rabi frequency.

The magnetic field interaction Hamiltonian H_B for a $\hat{\mathbf{z}}$ -directed magnetic field \mathbf{B} is given by

$$\begin{aligned} H_B &= -\boldsymbol{\mu} \cdot \mathbf{B} \\ &= g\mu_0 \mathbf{J} \cdot \mathbf{B} \\ &= g\mu_0 J_z B \\ &= \Omega_L \begin{pmatrix} -1 & 0 & 0 & 0 \\ 0 & 0 & 0 & 0 \\ 0 & 0 & 1 & 0 \\ 0 & 0 & 0 & 0 \end{pmatrix}, \end{aligned} \quad (10)$$

where Ω_L is the Larmor frequency as defined in Sec. I. Thus, the total Hamiltonian is given by

$$\begin{aligned} H &= H_0 + H_l + H_B \\ &= \begin{pmatrix} -\Omega_L & 0 & 0 & -2\Omega \cos \omega t \\ 0 & 0 & 0 & 0 \\ 0 & 0 & \Omega_L & 2\Omega \cos \omega t \\ -2\Omega \cos \omega t & 0 & 2\Omega \cos \omega t & \omega_0 \end{pmatrix}. \end{aligned} \quad (11)$$

C. Rotating-wave approximation

We now use the rotating-wave approximation in order to remove the optical-frequency time dependence from the Hamiltonian. We first transform into the frame rotating at the optical frequency by means of the unitary transformation operator $U(t) = \exp(-iH't)$, where

$$H' = \begin{pmatrix} 0 & 0 & 0 & 0 \\ 0 & 0 & 0 & 0 \\ 0 & 0 & 0 & 0 \\ 0 & 0 & 0 & \omega \end{pmatrix} \quad (12)$$

is the unperturbed Hamiltonian H_0 with ω_0 replaced by ω . It is straightforward to show that under this transformation the Hamiltonian in the rotating frame is given by

$$\begin{aligned} \tilde{H} &= U^{-1}(t) H(t) U(t) - i U^{-1}(t) \frac{d}{dt} U(t) \\ &= \begin{pmatrix} -\Omega_L & 0 & 0 & -\Omega(1 + e^{-2i\omega t}) \\ 0 & 0 & 0 & 0 \\ 0 & 0 & \Omega_L & \Omega(1 + e^{-2i\omega t}) \\ -\Omega(1 + e^{2i\omega t}) & 0 & \Omega(1 + e^{2i\omega t}) & \omega_0 - \omega \end{pmatrix}, \end{aligned} \quad (13)$$

where we have used $\cos \omega t = (e^{-i\omega t} + e^{i\omega t})/2$. Averaging over an optical cycle to remove far-off-resonant terms (the rotating wave approximation), we have

$$\tilde{H} \simeq \begin{pmatrix} -\Omega_L & 0 & 0 & -\Omega \\ 0 & 0 & 0 & 0 \\ 0 & 0 & \Omega_L & \Omega \\ -\Omega & 0 & \Omega & -\Delta \end{pmatrix}. \quad (14)$$

where $\Delta = \omega - \omega_0$ is the (time-dependent) optical detuning.

D. Relaxation and repopulation

We assume that the upper state spontaneously decays with a rate γ_0 , and that the ground state relaxes with a rate γ , due to the exit of atoms from the light beam, in the case of the “transit” effect, or collisions with other atoms or the cell wall in the case of the “wall-induced Ramsey effect” [1]. (Additional upper-state relaxation processes can be neglected in comparison with the spontaneous decay rate.) This relaxation is described by the matrix Γ , given by

$$\Gamma = \begin{pmatrix} \gamma & 0 & 0 & 0 \\ 0 & \gamma & 0 & 0 \\ 0 & 0 & \gamma & 0 \\ 0 & 0 & 0 & \gamma_0 \end{pmatrix}. \quad (15)$$

The simplest model of ground state relaxation is used. The effects of collisional dephasing could be included by adding off-diagonal terms if a more realistic model is desired. In order to conserve the number of atoms, the

ground state must be replenished at the same rate at which it relaxes. This is described by the repopulation matrix Λ :

$$\Lambda = \frac{N}{3} \begin{pmatrix} \gamma & 0 & 0 & 0 \\ 0 & \gamma & 0 & 0 \\ 0 & 0 & \gamma & 0 \\ 0 & 0 & 0 & 0 \end{pmatrix}, \quad (16)$$

where N is the atomic density. We ignore repopulation due to spontaneous decay since the calculation is performed in the low-light-power limit ($\Omega^2 \ll \gamma_0\gamma$).

E. Density-matrix evolution equations

The evolution of the density matrix ρ (defined so that $\text{Tr } \rho = N$) is given by the Liouville equation [22]

$$\dot{\rho} = -i [\tilde{H}, \rho] - \frac{1}{2} \{\Gamma, \rho\} + \Lambda, \quad (17)$$

where the square brackets denote the commutator and the curly brackets the anticommutator. The $M = 0$ ground-state sublevel does not couple to the light, and can be ignored. Using $|1\rangle$ and $|2\rangle$ to denote the ground-state $M = -1$ and $+1$ sublevels, respectively, and $|3\rangle$ to denote the upper state, and assuming that $\gamma \ll \gamma_0$, the evolution equations for the atomic coherences obtained from Eq. (17) are

$$\dot{\rho}_{31} = -[\gamma_0/2 + i(\Omega_L - \Delta)] \rho_{31} + i\Omega(\rho_{11} - \rho_{33} - \rho_{21}), \quad (18a)$$

$$\dot{\rho}_{23} = -[\gamma_0/2 + i(\Omega_L + \Delta)] \rho_{23} + i\Omega(\rho_{22} - \rho_{33} - \rho_{21}), \quad (18b)$$

$$\dot{\rho}_{21} = -(\gamma + 2i\Omega_L) \rho_{21} - i\Omega(\rho_{31} + \rho_{23}). \quad (18c)$$

We can assume that in the low-light-power limit the populations $\rho_{11,22,33}$ are essentially unperturbed by the light ($\rho_{11,22} \simeq N/3$, $\rho_{33} \ll N$). We can also assume that, neglecting transient terms, the optical coherences $\rho_{31,23}$ are slowly varying (any time dependence would be due to modulation of the light frequency, which will always be done at a rate much less than γ_0 ; thus $\dot{\rho}_{31,23} \ll \gamma_0 \rho_{31,23}$). Using these assumptions, the evolution equations for the atomic coherences [Eqs. (18a–18c)] become

$$0 \simeq -[\gamma_0/2 + i(\Omega_L - \Delta)] \rho_{31} + i\Omega(N/3 - \rho_{21}), \quad (19a)$$

$$0 \simeq -[\gamma_0/2 + i(\Omega_L + \Delta)] \rho_{23} + i\Omega(N/3 - \rho_{21}), \quad (19b)$$

$$\dot{\rho}_{21} \simeq -(\gamma + 2i\Omega_L) \rho_{21} - i\Omega(\rho_{31} + \rho_{23}). \quad (19c)$$

These equations can be used to solve for the optical and ground-state coherences.

F. Calculation of the optical and ground-state coherences

The expression for optical rotation (Sec. III H) is written in terms of the optical coherences $\rho_{31,23}$. We will now

relate the optical coherences to the ground-state coherence ρ_{21} and find an expression for ρ_{21} as a sum over harmonics of the light detuning modulation frequency Ω_m . This form is convenient because the signal is measured at harmonics of this frequency.

Solving Eqs. (19a) and (19b) for ρ_{31} and ρ_{23} in terms of ρ_{21} , we obtain

$$\begin{aligned}\rho_{31} &\simeq \frac{\Omega(N/3 - \rho_{21})}{\Omega_L - \Delta - i\gamma_0/2}, \\ \rho_{23} &\simeq \frac{\Omega(N/3 - \rho_{21})}{\Omega_L + \Delta - i\gamma_0/2}.\end{aligned}\quad (20)$$

In order to solve for ρ_{21} , we make the substitution $\rho_{21} \rightarrow r_{21}e^{-(2i\Omega_L + \gamma)t}$ in Eq. (19c):

$$\dot{r}_{21} \simeq -i\Omega(\rho_{31} + \rho_{23})e^{(2i\Omega_L + \gamma)t}, \quad (21)$$

or, integrating (assuming that $r_{21} = \rho_{21} = 0$ at $t = 0$),

$$r_{21} \simeq -i\Omega \int_0^t (\rho_{31} + \rho_{23})e^{(2i\Omega_L + \gamma)\tau} d\tau, \quad (22)$$

so, substituting back,

$$\rho_{21} \simeq -i\Omega \int_0^t (\rho_{31} + \rho_{23})e^{-(2i\Omega_L + \gamma)(t-\tau)} d\tau. \quad (23)$$

The expressions for the optical coherences [Eqs. (20)] are then substituted into the expression for the ground-state coherence [Eq. (23)]. Assuming that the light power is low ($\Omega \ll \gamma_0$) allows us to neglect second-order terms. We also assume that the level shift induced by the magnetic field is smaller than the natural line width, i.e. $\Omega_L \ll \gamma_0$. (For the D -lines of rubidium used in the experiment, this assumption holds for magnetic fields up to the earth-field range.) The ground-state coherence is then given by

$$\begin{aligned}\rho_{21} &\simeq -\frac{i}{3}\Omega^2 N \int_0^t \left(\frac{1}{\Omega_L - \Delta - i\gamma_0/2} + \frac{1}{\Omega_L + \Delta - i\gamma_0/2} \right) \\ &\quad \times e^{-(2i\Omega_L + \gamma)(t-\tau)} d\tau \\ &\simeq \frac{2}{3}\Omega^2 N \int_0^t \left(\frac{\gamma_0/2 - i\Omega_L}{\Delta^2 + \gamma_0^2/4} + \frac{2i\Omega_L\Delta^2}{(\Delta^2 + \gamma_0^2/4)^2} \right) \\ &\quad \times e^{-(2i\Omega_L + \gamma)(t-\tau)} d\tau \\ &= \frac{2}{3}\Omega^2 N [(\gamma_0/2 - i\Omega_L) I_1(t) + 2i\Omega_L I_2(t)],\end{aligned}\quad (24)$$

where the integral I_1 has been defined by

$$\begin{aligned}I_1(t) &= \int_0^t \frac{e^{-(2i\Omega_L + \gamma)(t-\tau)} d\tau}{\Delta_0^2 (D_0 - \cos \Omega_m \tau)^2 + \gamma_0^2/4} \\ &= (\gamma_0^2/4)^{-1} \int_0^t f(\Omega_m \tau) e^{-(2i\Omega_L + \gamma)(t-\tau)} d\tau,\end{aligned}\quad (25)$$

and I_2 has been defined by

$$\begin{aligned}I_2(t) &= \int_0^t \frac{\Delta_0^2 (D_0 - \cos \Omega_m \tau)^2 d\tau}{\left[\Delta_0^2 (D_0 - \cos \Omega_m \tau)^2 + \gamma_0^2/4 \right]^2} e^{-(2i\Omega_L + \gamma)(t-\tau)} \\ &= -\Delta_0^2 \frac{\partial I_1(t)}{\partial \Delta_0^2}.\end{aligned}\quad (26)$$

Here we have substituted for Δ the expression for the light-frequency modulation $\Delta = \Delta_0 (D_0 - \cos \Omega_m \tau)$, where the dimensionless average detuning parameter D_0 is defined by $D_0 = \Delta_l/\Delta_0$, where $\Delta_l = \omega_l - \omega_0$. The lineshape factor $f(x)$ is defined by

$$f(x) = \frac{\gamma_0^2/4}{\Delta_0^2 (D_0 - \cos x)^2 + \gamma_0^2/4}. \quad (27)$$

Expanding this function as a series of harmonics,

$$f(x) = \sum_{n=-\infty}^{\infty} a_n e^{inx}, \quad (28)$$

the coefficients a_n are given by

$$a_n = \frac{1}{2\pi} \int_{-\pi}^{\pi} f(x) \cos nx dx. \quad (29)$$

Substituting the series expansion for $f(x)$ into I_1 , we have

$$\begin{aligned}I_1(t) &\simeq \int_0^t \left[(\gamma_0^2/4)^{-1} \sum_{n=-\infty}^{\infty} a_n e^{in\Omega_m \tau} \right] e^{-(2i\Omega_L + \gamma)(t-\tau)} d\tau \\ &= (\gamma_0^2/4)^{-1} \sum_{n=-\infty}^{\infty} \frac{e^{in\Omega_m t} - e^{-(\gamma + 2i\Omega_L)t}}{\gamma + i(2\Omega_L + n\Omega_m)} a_n \\ &\simeq (\gamma_0^2/4)^{-1} \sum_{n=-\infty}^{\infty} \frac{a_n e^{in\Omega_m t}}{\gamma + i(2\Omega_L + n\Omega_m)},\end{aligned}\quad (30)$$

where we have discarded the transient term $e^{-(\gamma + 2i\Omega_L)t}$. The expression for I_2 [Eq. (26)] can be found from that for I_1 :

$$\begin{aligned}I_2(t) &= -\Delta_0^2 \frac{\partial I_1(t)}{\partial \Delta_0^2} \\ &\simeq (\gamma_0^2/4)^{-1} \sum_{n=-\infty}^{\infty} \frac{b_n e^{in\Omega_m t}}{\gamma + i(2\Omega_L + n\Omega_m)},\end{aligned}\quad (31)$$

where the coefficient b_n is defined by

$$b_n = -\Delta_0^2 \frac{\partial a_n}{\partial \Delta_0^2} \quad (32)$$

In order to find the relative values of a_n and b_n , it is useful to have an approximate expression for them. Assuming

that $\gamma_0 \ll \Delta_0$, we can replace $f(x)$ with a delta function normalized to the same area:

$$f(x) \simeq \frac{\pi\gamma_0}{2\Delta_0\sqrt{1-D_0^2}} \delta(D_0 - \cos x). \quad (33)$$

Substituting this expression into Eq. (29), we obtain

$$a_n \simeq \frac{\gamma_0}{2\Delta_0} \frac{\cos(n \arccos D_0)}{\sqrt{1-D_0^2}}. \quad (34)$$

This approximation breaks down for $|D_0|$ within $\sim \gamma_0/\Delta_0$ of unity. However, as we see below, we are interested in integrals of a_n over effective detuning, which can be well approximated using the expression (34). We are also limited by this approximation to harmonics $n \ll \Delta_0/\gamma_0$, since the factor $\cos nx$ is assumed to not vary rapidly over the optical resonance. Thus, from Eq. (32), b_n can be approximated by

$$\begin{aligned} b_n &\simeq \frac{\gamma_0}{4\Delta_0} \frac{\cos(n \arccos D_0)}{\sqrt{1-D_0^2}} \\ &\simeq \frac{1}{2} a_n. \end{aligned} \quad (35)$$

Thus we see that $I_2 \simeq I_1/2$ and the terms of Eq. (24) proportional to Ω_L cancel. Substituting Eq. (30) into Eq. (24), we obtain

$$\rho_{21} \simeq \frac{4\Omega^2 N}{3\gamma_0} \sum_{n=-\infty}^{\infty} \frac{a_n e^{in\Omega_m t}}{\gamma + i(2\Omega_L + n\Omega_m)}. \quad (36)$$

The result (36) applies to atoms that are at rest. We now modify this result to describe an atomic ensemble with a Maxwellian velocity distribution leading to a Doppler width Γ_D of the transition. For an atomic velocity group with component of velocity v along the light propagation direction, the light frequency is shifted according to $\omega(v) = \omega(1 - v/c) = \omega - kv$ where k is the light-field wave number. Writing the dimensionless Doppler-shift parameter $D_v = -kv/\Delta_0$, the atomic density N for this velocity group becomes

$$dN(v) = \frac{\Delta_0}{\Gamma_D \sqrt{\pi}} N_0 e^{-(D_v \Delta_0 / \Gamma_D)^2} dD_v, \quad (37)$$

where N_0 is the total atomic density, and the average detuning parameter D_0 becomes $D_0(v) = D_0 + D_v$. Defining the velocity-dependent coefficient $a_n(v)$ by

$$\begin{aligned} a_n(v) dD_v &= \frac{\Gamma_D}{\gamma_0} \frac{dN(v)}{N_0} a_n \\ &\simeq \frac{\cos[n \arccos(D_0 + D_v)]}{2\sqrt{\pi} \sqrt{1 - (D_0 + D_v)^2}} e^{-(D_v \Delta_0 / \Gamma_D)^2} dD_v, \end{aligned} \quad (38)$$

the velocity-dependent ground-state coherence $\rho_{21}(v)$ is

given by

$$\begin{aligned} \rho_{21}(v) dD_v &\simeq \frac{4\Omega^2 dN(v)}{3\gamma_0} \sum_{n=-\infty}^{\infty} \frac{a_n e^{in\Omega_m t}}{\gamma + i(2\Omega_L + n\Omega_m)} \\ &\simeq \frac{4\Omega^2 N_0}{3\Gamma_D} \sum_{n=-\infty}^{\infty} \frac{a_n(v) e^{in\Omega_m t}}{\gamma + i(2\Omega_L + n\Omega_m)} dD_v. \end{aligned} \quad (39)$$

In a situation in which atomic collisions are important, such as in a vapor cell with a buffer gas or an antirelaxation coating, this result must be further modified to take into account collisionally induced velocity mixing. For atoms contained in an antirelaxation-coated vapor cell, we assume that each velocity group interacts separately with the excitation light, but after pumping all groups are completely mixed. This model applies when light power is low enough so that optical pumping averaged over the atomic velocity distribution and the cell volume is unsaturated. The ground-state coherence of each velocity group becomes the velocity-averaged quantity $\bar{\rho}_{21}(v)$, given by the normalized velocity average of Eq. (39):

$$\begin{aligned} \bar{\rho}_{21}(v) dD_v &\simeq \frac{dN(v)}{N_0} \int_{-\infty}^{\infty} \rho_{21}(v) dD_v \\ &= \frac{4\Omega^2 dN(v)}{3\Gamma_D} \sum_{n=-\infty}^{\infty} \frac{\bar{a}_n e^{in\Omega_m t}}{\gamma + i(2\Omega_L + n\Omega_m)}, \end{aligned} \quad (40)$$

where the averaged coefficient \bar{a}_n is given by

$$\begin{aligned} \bar{a}_n &= \int_{-\infty}^{\infty} a_n(v) dD_v \\ &\simeq \int_{-\infty}^{\infty} \frac{\cos[n \arccos(D_0 + D_v)]}{2\sqrt{\pi} \sqrt{1 - (D_0 + D_v)^2}} e^{-(D_v \Delta_0 / \Gamma_D)^2} dD_v. \end{aligned} \quad (41)$$

Below, we will need the real and imaginary parts of $\bar{\rho}_{21}$, given by

$$\begin{aligned} \text{Re } \bar{\rho}_{21}(v) dD_v &\simeq \frac{4\Omega^2 dN(v)}{3\Gamma_D} \\ &\times \sum_{n=-\infty}^{\infty} \frac{\bar{a}_n [\gamma \cos n\Omega_m t + (2\Omega_L + n\Omega_m) \sin n\Omega_m t]}{\gamma^2 + (2\Omega_L + n\Omega_m)^2}, \\ \text{Im } \bar{\rho}_{21}(v) dD_v &\simeq \frac{4\Omega^2 dN(v)}{3\Gamma_D} \\ &\times \sum_{n=-\infty}^{\infty} \frac{\bar{a}_n [\gamma \sin n\Omega_m t - (2\Omega_L + n\Omega_m) \cos n\Omega_m t]}{\gamma^2 + (2\Omega_L + n\Omega_m)^2}. \end{aligned} \quad (42)$$

G. Optical properties of the medium

We now derive the formula for the optical rotation in terms of the polarization of the medium $\mathbf{P} = \text{Tr } \rho \mathbf{d}$. The

electric field of coherent light of arbitrary polarization can be described by [23]

$$\mathbf{E} = \frac{1}{2} \left[E_0 e^{i\phi} (\cos \varphi \cos \epsilon - i \sin \varphi \sin \epsilon) e^{i(\omega t - kz)} + c.c. \right] \hat{\mathbf{e}}_x + \frac{1}{2} \left[E_0 e^{i\phi} (\sin \varphi \cos \epsilon + i \cos \varphi \sin \epsilon) e^{i(\omega t - kz)} + c.c. \right] \hat{\mathbf{e}}_y, \quad (43)$$

where $k = \omega/c$ is the vacuum wave number, ϕ is the overall phase, φ is the polarization angle, and ϵ is the ellipticity.

Substituting Eq. (43) into the wave equation

$$\left(\frac{d^2}{dz^2} - \frac{d^2}{c^2 dt^2} \right) \mathbf{E} = -\frac{4\pi}{c^2} \frac{d^2}{dt^2} \mathbf{P}, \quad (44)$$

and neglecting terms involving second-order derivatives and products of first-order derivatives (thus assuming that changes in φ , ϵ , and ϕ and fractional changes in E_0 are small), gives the rotation, phase shift, absorption, and change of ellipticity per unit distance:

$$\begin{aligned} \frac{d\varphi}{dz} &= -\frac{2\pi\omega}{E_0 c} \sec 2\epsilon [\cos \varphi (P_1 \sin \epsilon + P_4 \cos \epsilon) \\ &\quad - \sin \varphi (P_2 \cos \epsilon - P_3 \sin \epsilon)], \\ \frac{d\phi}{dz} &= -\frac{2\pi\omega}{E_0 c} \sec 2\epsilon [\cos \varphi (P_1 \cos \epsilon + P_4 \sin \epsilon) \\ &\quad - \sin \varphi (P_2 \sin \epsilon - P_3 \cos \epsilon)], \\ \frac{dE_0}{dz} &= \frac{2\pi\omega}{c} [\sin \varphi (P_1 \sin \epsilon - P_4 \cos \epsilon) \\ &\quad - \cos \varphi (P_2 \cos \epsilon + P_3 \sin \epsilon)], \\ \frac{d\epsilon}{dz} &= \frac{2\pi\omega}{E_0 c} [\sin \varphi (P_1 \cos \epsilon + P_4 \sin \epsilon) \\ &\quad + \cos \varphi (P_2 \sin \epsilon - P_3 \cos \epsilon)], \end{aligned} \quad (45)$$

where the components $P_{1,2,3,4}$ of the polarization are defined by

$$\mathbf{P} = \frac{1}{2} \left[(P_1 - iP_2) e^{i(\omega t - kz)} + c.c. \right] \hat{\mathbf{e}}_x + \frac{1}{2} \left[(P_3 - iP_4) e^{i(\omega t - kz)} + c.c. \right] \hat{\mathbf{e}}_y. \quad (46)$$

For initial values of $\varphi = \epsilon = 0$, the rotation per unit length is given by

$$\frac{d\varphi}{d\ell} = -\frac{2\pi\omega P_4}{cE_0}. \quad (47)$$

H. Calculation of the signal

We now evaluate $\mathbf{P} = \text{Tr} \rho \mathbf{d}$ and substitute into Eq. (47) to find the optical rotation in terms of the ground-state atomic coherence derived above. Taking into account that in the nonrotating frame the optical atomic coherences oscillate at the light frequency ω , we find for the polarization components

$$\begin{aligned} P_1 &= \sqrt{\frac{2}{3}} (\xi_g J_g \|d\| \xi_e J_e) \text{Re} (\rho_{31} - \rho_{23}), \\ P_2 &= -\sqrt{\frac{2}{3}} (\xi_g J_g \|d\| \xi_e J_e) \text{Im} (\rho_{31} + \rho_{23}), \\ P_3 &= -\sqrt{\frac{2}{3}} (\xi_g J_g \|d\| \xi_e J_e) \text{Im} (\rho_{31} - \rho_{23}), \\ P_4 &= -\sqrt{\frac{2}{3}} (\xi_g J_g \|d\| \xi_e J_e) \text{Re} (\rho_{31} + \rho_{23}), \end{aligned} \quad (48)$$

so the optical rotation angle per unit length is given by

$$\begin{aligned} \frac{d\varphi}{d\ell} &= \frac{\pi\omega (\xi_g J_g \|d\| \xi_e J_e)^2}{3\Omega c} \text{Re} (\rho_{31} + \rho_{32}) \\ &= \frac{\gamma_0 \lambda^2}{16\pi\Omega} \text{Re} (\rho_{31} + \rho_{32}), \end{aligned} \quad (49)$$

where λ is the transition wavelength. Here we have used the fact that for a closed $J \rightarrow J'$ transition [21],

$$\gamma_0 = \frac{4\omega_0^3}{3c^3} \frac{1}{2J' + 1} (\xi J \|d\| \xi' J')^2, \quad (50)$$

and that $\omega \simeq \omega_0$.

Substituting in the expressions (20), and assuming $\rho_{11} \simeq \rho_{22} \simeq N/3$ and $\Omega_L \ll \gamma_0$, Eq. (49) can be written in terms of the ground-state coherence as

$$\frac{d\varphi}{d\ell} = \frac{\gamma_0 \lambda^2}{8\pi} \left(\frac{\Omega_L (N/3 - \text{Re} \rho_{21}) + (\gamma_0/2) \text{Im} \rho_{21}}{\gamma_0^2/4 + \Delta^2} - \frac{2\Omega_L \Delta^2 (N/3 - \text{Re} \rho_{21})}{(\gamma_0^2/4 + \Delta^2)^2} \right), \quad (51)$$

or, for the case of complete velocity mixing:

$$\frac{d\varphi(v)}{d\ell} dD_v = \frac{\gamma_0 \lambda^2}{8\pi} \left(\frac{\Omega_L [dN(v)/3 - \text{Re} \bar{\rho}_{21}(v) dD_v] + (\gamma_0/2) \text{Im} \bar{\rho}_{21}(v) dD_v}{\gamma_0^2/4 + \Delta^2(v)} - \frac{2\Omega_L \Delta^2(v) [dN(v)/3 - \text{Re} \bar{\rho}_{21}(v) dD_v]}{[\gamma_0^2/4 + \Delta^2(v)]^2} \right), \quad (52)$$

where the velocity-dependent effective detuning $\Delta(v)$ is

given, as before, by

$$\Delta(v) = \Delta_0 [D_0(v) - \cos \Omega_m \tau]. \quad (53)$$

The in-phase and quadrature signals (see Sec. II) per unit length of the medium, measured for a time T at the j -th harmonic of the modulation frequency, are given by the time averages

$$\begin{aligned}\frac{d\varphi_j^{\text{in}}(v)}{d\ell} dD_v &= \frac{dD_v}{T} \int_0^T \frac{d\varphi(v)}{d\ell} \cos(j\Omega_m t) dt, \\ \frac{d\varphi_j^{\text{out}}(v)}{d\ell} dD_v &= \frac{dD_v}{T} \int_0^T \frac{d\varphi(v)}{d\ell} \sin(j\Omega_m t) dt.\end{aligned}\quad (54)$$

We substitute the formulas for the real and imaginary parts of the ground-state coherence [Eq. (42)] into the formula for the optical rotation [Eq. (52)], and the resulting expression into Eq. (54). After evaluating the time integrals (see Appendix A), we find that the signals due to each velocity group are given by

$$\begin{aligned}\frac{d\varphi_j^{\text{in}}(v)}{d\ell} dD_v &\simeq -\frac{\lambda^2 \Omega^2}{6\pi\Gamma_D} dN(v) \\ &\quad \times \sum_{n=-\infty}^{\infty} \frac{(2\Omega_L + n\Omega_m) \bar{a}_n (a_{n+j} + a_{n-j})}{\gamma^2 + (2\Omega_L + n\Omega_m)^2}, \\ \frac{d\varphi_j^{\text{out}}(v)}{d\ell} dD_v &\simeq -\frac{\lambda^2 \Omega^2}{6\pi\Gamma_D} dN(v) \\ &\quad \times \sum_{n=-\infty}^{\infty} \frac{\gamma \bar{a}_n (a_{n+j} - a_{n-j})}{\gamma^2 + (2\Omega_L + n\Omega_m)^2}.\end{aligned}\quad (55)$$

Using the definitions of $dN(v)$ and $a_n(v)$ [Eqs. (37,38)] we can rewrite Eq. (55) as

$$\begin{aligned}\frac{d\varphi_j^{\text{in}}(v)}{d\ell} dD_v &\simeq \eta \sum_{n=-\infty}^{\infty} \frac{\gamma (2\Omega_L + n\Omega_m) \bar{a}_n [a_{n+j}(v) + a_{n-j}(v)]}{\gamma^2 + (2\Omega_L + n\Omega_m)^2} dD_v, \\ \frac{d\varphi_j^{\text{out}}(v)}{d\ell} dD_v &\simeq \eta \sum_{n=-\infty}^{\infty} \frac{\gamma^2 \bar{a}_n [a_{n+j}(v) - a_{n-j}(v)]}{\gamma^2 + (2\Omega_L + n\Omega_m)^2} dD_v,\end{aligned}\quad (56)$$

where the signal amplitude factor η is defined by

$$\eta = -\frac{1}{6\pi} \frac{\Omega^2 \gamma_0}{\Gamma_D^2 \gamma} \lambda^2 N_0. \quad (57)$$

The total signal, given by the integral over all velocity

groups, is found by replacing $a_n(v)$ with \bar{a}_n :

$$\begin{aligned}\left. \frac{d\varphi_j^{\text{in}}}{d\ell} \right|_{\text{total}} &= \int_{-\infty}^{\infty} \frac{d\varphi_j^{\text{in}}(v)}{d\ell} dD_v \\ &\simeq \eta \sum_{n=-\infty}^{\infty} \frac{\gamma (2\Omega_L + n\Omega_m) \bar{a}_n (\bar{a}_{n+j} + \bar{a}_{n-j})}{\gamma^2 + (2\Omega_L + n\Omega_m)^2}, \\ \left. \frac{d\varphi_j^{\text{out}}}{d\ell} \right|_{\text{total}} &= \int_{-\infty}^{\infty} \frac{d\varphi_j^{\text{out}}(v)}{d\ell} dD_v \\ &\simeq \eta \sum_{n=-\infty}^{\infty} \frac{\gamma^2 \bar{a}_n (\bar{a}_{n+j} - \bar{a}_{n-j})}{\gamma^2 + (2\Omega_L + n\Omega_m)^2}.\end{aligned}\quad (58)$$

Each term of the sums corresponds to a resonance at $\Omega_L/\Omega_m = -n/2$ (Figs. 3,4). Near each resonance the in-phase signal is dispersive in shape, whereas the quadrature signal is a Lorentzian. When plotted as a function of the Larmor frequency normalized to the modulation frequency, Ω_L/Ω_m , the widths of the resonances are determined by the normalized ground-state relaxation rate γ/Ω_m . The relative amplitudes of the resonances are determined by the ratio of the modulation depth to the Doppler width, Δ_0/Γ_D , and the normalized average detuning Δ_l/Δ_0 .

IV. CONCLUSION

We have presented a theory of nonlinear magneto-optical rotation with low-power frequency-modulated light for a low-angular-momentum system. The magnetic-field dependence predicted by this theory is in qualitative agreement with experimental data taken on the Rb $D1$ line. Directions for future work include a more complete theory describing higher-angular-momentum systems, including systems with hyperfine structure, and higher light powers. A possible complication to the FM NMOR technique in systems with hyperfine structure is the nonlinear Zeeman effect present at higher magnetic fields, so a theoretical description of this effect would also be helpful. FM NMOR has been shown to be a useful technique for the selective study of higher-order polarization moments, which give rise to distinct resonances at different values of the magnetic field than the quadrupole resonances studied here [8] (see also Ref. [24]). Higher-order moments are of interest in part because signals due to the highest-order moments possible in a given system would be free of the complications due to the nonlinear Zeeman effect. To describe these moments, a calculation along the same lines as the one presented here but carried out to higher order and involving more atomic sublevels would be necessary.

Acknowledgments

We thank M. Auzinsh, W. Gawlik, and A. Lezama for helpful discussions. This work has been supported by the Office of Naval Research (grant N00014-97-1-0214); by a US-Armenian bilateral Grant CRDF AP2-3213/NFSAT PH 071-02; by NSF; by the Director, Office of Science, Nuclear Science Division, of the U.S. Department of Energy under contract DE-AC03-76SF00098; and by a CalSpace Minigrant. D.B. also acknowledges the support of the Miller Institute for Basic Research in Science.

APPENDIX A: EVALUATION OF THE TIME INTEGRALS

In evaluating Eq. (54), several time integrals appear:

$$I_3 = \frac{1}{\Omega_m T} \int_0^{\Omega_m T} \frac{\cos jx}{\gamma_0^2/4 + \Delta_0^2 [D_0(v) - \cos x]^2} dx,$$

$$I_4 = \frac{1}{\Omega_m T} \int_0^{\Omega_m T} \frac{\sin jx}{\gamma_0^2/4 + \Delta_0^2 [D_0(v) - \cos x]^2} dx,$$

$$I_5 = \frac{1}{\Omega_m T} \int_0^{\Omega_m T} \frac{\cos jx \sin nx}{\gamma_0^2/4 + \Delta_0^2 [D_0(v) - \cos x]^2} dx,$$

$$I_6 = \frac{1}{\Omega_m T} \int_0^{\Omega_m T} \frac{\sin jx \sin nx}{\gamma_0^2/4 + \Delta_0^2 [D_0(v) - \cos x]^2} dx,$$

$$I_7 = \frac{1}{\Omega_m T} \int_0^{\Omega_m T} \frac{\cos jx \cos nx}{\gamma_0^2/4 + \Delta_0^2 [D_0(v) - \cos x]^2} dx,$$

$$I_8 = \frac{1}{\Omega_m T} \int_0^{\Omega_m T} \frac{\sin jx \cos nx}{\gamma_0^2/4 + \Delta_0^2 [D_0(v) - \cos x]^2} dx,$$

as well as the related integrals

$$I_9 = \frac{1}{\Omega_m T} \int_0^{\Omega_m T} \frac{\Delta_0^2 [D_0(v) - \cos x]^2 \cos jx}{\left\{ \gamma_0^2/4 + \Delta_0^2 [D_0(v) - \cos x]^2 \right\}^2} dx$$

$$= -\Delta_0^2 \frac{\partial I_3}{\partial \Delta_0^2},$$

$$I_{10} = \frac{1}{\Omega_m T} \int_0^{\Omega_m T} \frac{\Delta_0^2 [D_0(v) - \cos x]^2 \sin jx}{\left\{ \gamma_0^2/4 + \Delta_0^2 [D_0(v) - \cos x]^2 \right\}^2} dx$$

$$= -\Delta_0^2 \frac{\partial I_4}{\partial \Delta_0^2},$$

$$I_{11} = \frac{1}{\Omega_m T} \int_0^{\Omega_m T} \frac{\Delta_0^2 [D_0(v) - \cos x]^2 \cos jx \sin nx}{\left\{ \gamma_0^2/4 + \Delta_0^2 [D_0(v) - \cos x]^2 \right\}^2} dx$$

$$= -\Delta_0^2 \frac{\partial I_5}{\partial \Delta_0^2},$$

$$I_{12} = \frac{1}{\Omega_m T} \int_0^{\Omega_m T} \frac{\Delta_0^2 [D_0(v) - \cos x]^2 \sin jx \sin nx}{\left\{ \gamma_0^2/4 + \Delta_0^2 [D_0(v) - \cos x]^2 \right\}^2} dx$$

$$= -\Delta_0^2 \frac{\partial I_6}{\partial \Delta_0^2},$$

$$I_{13} = \frac{1}{\Omega_m T} \int_0^{\Omega_m T} \frac{\Delta_0^2 [D_0(v) - \cos x]^2 \cos jx \cos nx}{\left\{ \gamma_0^2/4 + \Delta_0^2 [D_0(v) - \cos x]^2 \right\}^2} dx$$

$$= -\Delta_0^2 \frac{\partial I_7}{\partial \Delta_0^2},$$

$$I_{14} = \frac{1}{\Omega_m T} \int_0^{\Omega_m T} \frac{\Delta_0^2 [D_0(v) - \cos x]^2 \sin jx \cos nx}{\left\{ \gamma_0^2/4 + \Delta_0^2 [D_0(v) - \cos x]^2 \right\}^2} dx$$

$$= -\Delta_0^2 \frac{\partial I_8}{\partial \Delta_0^2}.$$

If T is many modulation periods, the above integrals can be approximated by averages over one period. Thus, we can change the limits of the integrals to $(-\pi, \pi)$, and set the normalizing factor $(\Omega_m T)^{-1}$ to $(2\pi)^{-1}$. Using the trigonometric substitutions

$$\begin{aligned} \cos jx \cos nx &= \frac{1}{2} \{ \cos [(n-j)x] + \cos [(n+j)x] \}, \\ \cos jx \sin nx &= \frac{1}{2} \{ \sin [(n-j)x] + \sin [(n+j)x] \}, \\ \sin jx \sin nx &= \frac{1}{2} \{ \cos [(n-j)x] - \cos [(n+j)x] \}, \\ \sin jx \cos nx &= -\frac{1}{2} \{ \sin [(n-j)x] + \sin [(n+j)x] \}, \end{aligned} \tag{A1}$$

we can rewrite the above integrals in terms of the a_n and b_n coefficients.

$$\begin{aligned}
I_3 &\simeq (\gamma_0^2/4)^{-1} a_j, \\
I_4 &\simeq 0, \\
I_5 &\simeq 0, \\
I_6 &\simeq (\gamma_0^2/4)^{-1} \frac{(a_{n-j} - a_{n+j})}{2}, \\
I_7 &\simeq (\gamma_0^2/4)^{-1} \frac{(a_{n-j} + a_{n+j})}{2}, \\
I_8 &\simeq 0, \\
I_9 &\simeq (\gamma_0^2/4)^{-1} b_j, \\
I_{10} &\simeq 0, \\
I_{11} &\simeq 0, \\
I_{12} &\simeq (\gamma_0^2/4)^{-1} \frac{(b_{n-j} - b_{n+j})}{2}, \\
I_{13} &\simeq (\gamma_0^2/4)^{-1} \frac{(b_{n-j} + b_{n+j})}{2}, \\
I_{14} &\simeq 0.
\end{aligned} \tag{A2}$$

As in the evaluation of Eq. (24), use of the approximate expression $b_n \simeq a_n/2$ [Eq. (35)] results in the cancella-

tion of some terms proportional to Ω_L , producing the relatively simple form of Eq. (55).

-
- [1] D. Budker, W. Gawlik, D. F. Kimball, S. M. Rochester, V. V. Yashchuk, and A. Weis, *Rev. Mod. Phys.* **74**(4), 1153 (2002).
 - [2] D. Budker, D. J. Orlando, and V. Yashchuk, *Am. J. Phys.* **67**(7), 584 (1999).
 - [3] D. Budker, D. F. Kimball, S. M. Rochester, V. V. Yashchuk, and M. Zolotarev, *Phys. Rev. A* **62**(4), 043403 (2000).
 - [4] E. B. Alexandrov, M. V. Balabas, A. S. Pasgalev, A. K. Vershovskii, and N. N. Yakobson, *Laser Physics* **6**(2), 244 (1996).
 - [5] D. Budker, V. Yashchuk, and M. Zolotarev, *Phys. Rev. Lett.* **81**(26), 5788 (1998).
 - [6] P. Ripka, *Magnetic sensors and magnetometers*, Artech House remote sensing library (Artech House, Boston, 2001).
 - [7] D. Budker, D. F. Kimball, V. V. Yashchuk, and M. Zolotarev, *Phys. Rev. A* **65**, 055403 (2002).
 - [8] V. V. Yashchuk, D. Budker, W. Gawlik, D. F. Kimball, Y. P. Malakyan, and S. M. Rochester, *Phys. Rev. Lett.* **90**, 253001 (2003).
 - [9] L. M. Barkov and M. S. Zolotarev, *Pis'ma Zh. Éksp. Teor. Fiz.* **28**(8), 544 (1978).
 - [10] L. M. Barkov, M. Zolotarev, and D. A. Melik-Pashaev, *Pis'ma Zh. Éksp. Teor. Fiz.* **48**(3), 144 (1988).
 - [11] B. Cheron, H. Gilles, J. Hamel, O. Moreau, and E. Noel, *Opt. Commun.* **115**(1-2), 71 (1995).
 - [12] B. Cheron, H. Gilles, J. Hamel, O. Moreau, and E. Noel, *J. Phys. II* **6**(2), 175 (1996).
 - [13] H. Gilles, J. Hamel, and B. Cheron, *Rev. Sci. Instrum.* **72**(5), 2253 (2001).
 - [14] C. Andreeva, G. Bevilacqua, V. Biancalana, S. Cartaleva, Y. Dancheva, T. Karaulanov, C. Marinelli, E. Mariotti, and L. Moi, *Appl. Phys. B, Lasers Opt.* **76**(6), 667 (2003).
 - [15] P. Valente, H. Failache, and A. Lezama, *Phys. Rev. A* **67**(1), 13806 (2003).
 - [16] W. Bell and A. Bloom, *Phys. Rev. Lett.* **6**(6), 280 (1961).
 - [17] E. B. Aleksandrov, *Opt. Spectrosk.* **17**, 957 (1963).
 - [18] M. Auzinsh and R. Ferber, *Optical polarization of molecules*, vol. 4 of *Cambridge monographs on atomic, molecular, and chemical physics* (Cambridge University, Cambridge, England, 1995).
 - [19] M. V. Romalis, W. C. Griffith, J. P. Jacobs, and E. N. Fortson, *Phys. Rev. Lett.* **86**(12), 2505 (2001).
 - [20] M. V. Romalis, W. C. Griffith, J. P. Jacobs, and E. N. Fortson, in *Art and Symmetry in Experimental Physics: Festschrift for Eugene D. Commins*, edited by D. Budker, S. J. Freedman, and P. Bucksbaum (AIP, Melville, New York, 2001), vol. 596 of *AIP Conference Proceedings*, pp. 47–61.
 - [21] I. I. Sobelman, *Atomic Spectra and Radiative Transitions* (Springer, Berlin, 1992).
 - [22] M. O. Scully and M. S. Zubairy, *Quantum Optics* (Cambridge University, Cambridge, England, 1997).
 - [23] S. Huard, *Polarization of light* (Wiley, New York, 1997).
 - [24] M. P. Auzin'sh and R. S. Ferber, *Pis'ma Zh. Éksp. Teor. Fiz.* **39**(8), 376 (1984).